Atmos. Chem. Phys. Discuss., 12, 14927–14957, 2012
www.atmos-chem-phys-discuss.net/12/14927/2012/
doi:10.5194/acpd-12-14927-2012

Atmospheric Chemistry and Physics Discussions

Sensitivity of cirrus and mixed-phase clouds to the ice nuclei spectra in McRAS-AC: single column model simulations

R. Morales Betancourt[1], **D. Lee**[2,3], **L. Oreopoulos**[3], **Y. C. Sud**[3], **D. Barahona**[4], and **A. Nenes**[1,5]

[1]School of Earth and Atmospheric Sciences, Georgia Institute of Technology, Atlanta, Georgia, USA
[2]USRA Goddard Earth Sciences Technology and Research, 10211 Wincopin Circle, Suite 500, Columbia, Maryland 21044, USA
[3]NASA Goddard Space Flight Center, NASA/GSFC, Greenbelt, Maryland 20771, USA
[4]NASA Goddard Space Flight Center, I.M. Systems Group, Maryland, USA
[5]School of Chemical and Biomolecular Engineering, Georgia Institute of Technology, Atlanta, Georgia, USA

Received: 17 May 2012 – Accepted: 23 May 2012 – Published: 12 June 2012

Correspondence to: A. Nenes (athanasios.nenes@gatech.edu)

Published by Copernicus Publications on behalf of the European Geosciences Union.

Abstract

The salient features of mixed-phase and ice clouds in a GCM cloud scheme are examined using the ice formation parameterizations of Liu and Penner (LP) and Barahona and Nenes (BN). The performance of LP and BN ice nucleation parameterizations were assessed in the GEOS-5 AGCM using the McRAS-AC cloud microphysics framework in single column mode. Four dimensional assimilated data from the intensive observation period of ARM TWP-ICE campaign was used to drive the fluxes and lateral forcing. Simulation experiments where established to test the impact of each parameterization in the resulting cloud fields. Three commonly used IN spectra were utilized in the BN parameterization to described the availability of IN for heterogeneous ice nucleation. The results show large similarities in the cirrus cloud regime between all the schemes tested, in which ice crystal concentrations were within a factor of 10 regardless of the parameterization used. In mixed-phase clouds there are some persistent differences in cloud particle number concentration and size, as well as in cloud fraction, ice water mixing ratio, and ice water path. Contact freezing in the simulated mixed-phase clouds contributed to transfer liquid to ice efficiently, so that on average, the clouds were fully glaciated at $T \sim 260\,\mathrm{K}$, irrespective of the ice nucleation parameterization used. Comparison of simulated ice water path to available satellite derived observations were also performed, finding that all the schemes tested with the BN parameterization predicted average values of IWP within ±15 % of the observations.

1 Introduction

The role of atmospheric aerosols in modulating the atmospheric radiative balance, by directly scattering solar radiation, or indirectly, modifying cloud optical and microphysical properties, has received considerable attention during the last couple of decades. Soluble and insoluble aerosol species provide nucleation sites for the atmospheric water vapor to form liquid droplets (Cloud Condensation Nuclei, CCN), and ice crystals

(Ice Nuclei, IN), respectively. The important interactions between aerosol particles and cloud optical and physical properties operate at temporal and spatial scales unresolved by Global Climate Models (GCMs); their inclusion in climate simulations therefore relies on parameterizations. The importance of these aerosol–cloud interactions, and their potential impact on climate, makes their inclusion in climate models through accurate and physically based schemes a high priority (Intergovernmental Panel on Climate Change, 2007).

Aerosol indirect effects (AIE) in warm clouds have been long studied and implemented in atmospheric models (e.g., Penner et al., 2006), but less has been accomplished for cold clouds. Modifications to the number density and sizes of ice crystals not only strongly affect the radiative properties of ice-bearing clouds, but also impacts the development of precipitation (e.g., Lohmann and Diehl, 2005; Lohmann, 2002). The complexities associated with cold and mixed-phase clouds (due in part to the concurrent action of different freezing mechanisms, the high selectivity of the IN process, and the theoretical uncertainties associated with their description) have challenged the representation of such clouds in GCMs, most of which lack explicit ice microphysics (Lohmann and Feichter, 2005). As a result, even the sign of the radiative effects of aerosol-ice cloud interactions remains uncertain in climate simulations.

Important steps to improve the simple treatments of cold and mixed-phase cloud microphysics originally included in GCMs have been undertaken in recent years. For example, the partitioning of cloud condensate between ice and liquid water in mixed-phase clouds ($235\,\mathrm{K} \leq T \leq 273\,\mathrm{K}$) was typically represented by a temperature-only approach (e.g., DelGenio et al., 1996; Rasch and Kristjánsson, 1998). This approach has been progressively replaced by a less empirical and more physically-based representation, in which the deposition growth of cloud ice at the expense of the liquid water, the Bergeron-Findeisen process (Pruppacher and Klett, 1997), is taken into account (e.g., Rotstayn et al., 2000). This prognostic approach for condensate partitioning which includes explicit dependency of the deposition rate on microphysical variables such as ice content q_i, and ice crystal concentration, N_c, has been adopted by a variety of GCMs (Sud and Lee, 2007; Liu et al., 2007; Salzmann et al., 2010).

Another advancement in GCM cloud schemes is the implementation of two-moment cloud microphyisics, which include prognostic equations for the mass as well as the the number concentration of different hydrometeor categories (e.g., Seifert and Beheng, 2001, 2006; Morrison and Gettelman, 2008). This has permitted the prognostic computation of cloud particles sizes and ice deposition rate (e.g., Salzmann et al., 2010; Muhlbauer and Lohmann, 2009).

Estimates of the AIE on ice-bearing clouds require an adequate description of the aerosol-cloud coupling through the nucleation process. This is, the prognostic calculation of hydrometeor sizes should be done in a manner consistent to aerosol load changes and aerosol characteristics. However, an efficient and comprehensive representation of the current understanding of the ice nucleation process in the framework of a GCM has proven difficult. Most ice nucleation parameterizations rely on simple functions to determine how many ice crystals will be heterogeneously nucleated at a given set of environmental conditions. These relations describing the availability of IN, termed IN spectra, exhibit different level of complexity, ranging from saturation–dependent schemes (Meyers et al., 1992; Phillips et al., 2007) to IN spectra with aerosol-dependent parameters derived empirically (Phillips et al., 2008). Theory-based approaches have also lead to formulations of IN spectra with explicit dependence on aerosol number concentration, aerosol size distribution, and aerosol surface properties (Khvorostyanov and Curry, 2009; Barahona and Nenes, 2009b; Barahona, 2012). Most GCM microphysical schemes that account explicitly for aerosol effects represent ice nucleation assuming that there is no variation in ice nucleation properties within an aerosol species. In reality, there is large variability in the ice nucleation properties of aerosol populations, which contributes to the large uncertainty in the predicted IN concentrations.

Homogeneous freezing of solution droplets (i.e., without the presence of a solid aerosol phase) may occur only at temperatures below 235 K, the homogeneous

Title Page
Abstract Introduction
Conclusions References
Tables Figures
◂ ▸
Back Close
Full Screen / Esc
Printer-friendly Version
Interactive Discussion

freezing threshold T_{hom} (Pruppacher and Klett, 1997). For temperatures higher than T_{hom}, in which mixed-phase clouds typically exist, the presence of a solid phase is necessary for ice formation, and therefore only heterogeneous ice nucleation is active. Below T_{hom}, where ice-only clouds form, the supersaturation with respect to ice is the result of the competition between the rate of cooling of the cloud parcel and the condensation on the nucleated ice crystals. Therefore, it varies dynamically given the amount of IN present and the dynamical forcing available. Furthermore, since homogeneous and heterogeneous ice nucleation may occur simultaneously, the competition from both mechanisms and their impact on supersaturation further complicate the calculations. For this reason Lagrangian simulations have been used to develop solutions to the variable supersaturation problem (e.g., Lin et al., 2002), and fits to these numerical solutions have been used to develop ice nucleation parameterizations. A few such parameterizations have been developed (Kärcher and Lohmann, 2002, 2003; Liu and Penner, 2005), and have been implemented in GCM models (Hoose et al., 2010). Analytical solutions to this problem have been developed in which any IN spectra can be used (Barahona and Nenes, 2009b).

For the case of mixed-phase clouds, liquid water, water vapor, and ice are simultaneously present, and can exhibit complex dynamics (e.g., Korolev, 2007). For the coarse resolution of GCM cloud schemes, the simplifying assumption that the water vapor is saturated with respect to liquid water is sometimes made. The supersaturation with respect to ice, S_i, is therefore constrained by thermodynamic equilibrium rather than by the competition of cooling and condensation. With this assumption, it is sufficient to know the availability of IN (given by an IN spectrum) at S_i to compute the nucleation rate of ice crystals.

A number of studies have focused on the implementation and evaluation of new microphysical schemes in GCM simulations, including prognostic calculation of the ice fraction in mixed phase clouds, and using more physically-based ice nucleation schemes (Storelvmo et al., 2008; Sud and Lee, 2007; Liu et al., 2007; Salzmann et al., 2010). Curry and Khvorostyanov (2012) performed a comparison of some heterogeneous nucleations parameterizations in a single-column model for long lived mixed-phase arctic clouds. However, none of these studies have performed sensitivity analysis of the simulated mixed-phase and cirrus clouds fields to different IN spectra.

In this study, we use the parameterization of Barahona and Nenes (2009b), BN hereafter, in which the ice nucleation problem is treated in a general framework that admits the use of any IN spectra, empirical or theoretical. Barahona et al. (2010) used the BN parameterization to compare common formulations of the IN spectrum in a chemical transport model, finding that the 2 to 3 orders of magnitude variation in the IN concentrations among different schemes would lead to up to a factor of 20 variation in N_c in cirrus clouds. The sensitivity can be even larger in mixed-phase clouds where only heterogeneous ice nucleation is active, and competition for water vapor does not buffer the response of crystal number to IN concentration changes.

Testing the impact of IN spectra in a comprehensive cloud microphysical framework would provide valuable information on how the uncertainties associated with ice nucleation are reflected on the cloud field variables when coupled to other cloud processes. In this study, we report the implementation of the BN ice nucleation scheme into the Microphysics of Clouds with Relaxed Arakawa-Schubert and Aerosol-Cloud interaction (McRAS-AC) (Sud and Lee, 2007) driven by the Goddard Earth Observing System Model, version 5 (GEOS-5). The flexibility provided by the BN ice nucleation parameterization is ideal for testing the sensitivity of the simulated cloud properties to the representation of IN spectra in the McRAS-AC framework. To isolate the response from the underlying physical parameterization, all the simulations were performed in the Single Column Model version of GEOS-5. This is a common test of GCM microphysics since the SCM configuration contains the same physical parameterizations as the host GCM model, with the advantage of a much smaller computational burden, and the laterally constrained input flux fields allows better delineation of the role of microphysical processes of cloud formation and aerosol effects. The simulations were forced with data collected during the Tropical Warm Pool International Cloud Experiment (TWP-ICE) intensive observation period (IOP) of the ARM program (May et al., 2008).

2 Model description and simulation set-up

A detailed description of the McRAS-AC microphysics can be found elsewhere (Sud and Walker, 1999; Sud and Lee, 2007; Bhattacharjee et al., 2010). Here we will primarily focus on describing the treatment of cold and mixed-phase clouds microphysics in McRAS-AC.

2.1 Ice nucleation in McRAS-AC

McRAS-AC has the option to invoke the Liu and Penner (2005), (LP), or the Barahona and Nenes (2008, 2009a,b) parameterizations to describe the ice nucleation process. This possibility was used to assess and compare the performance of the two schemes. The LP parameterization was originally designed to describe the nucleation process at temperatures typical of cirrus cloud formation, i.e., for temperature less than the homogeneous freezing threshold ($T_{\mathrm{hom}} = 235\,\mathrm{K}$). It is based on numerical correlations derived from statistical fits to a large number of Lagrangian parcel model simulations, in which homogeneous and heterogeneous freezing mechanisms were explicitly accounted for. The homogeneous freezing of deliquesced sulfate aerosol was approached using an effective freezing temperature. Immersion freezing on soot particles was included in the parcel model simulations using a classical nucleation theory description, in which a fixed aerosol size distribution and freezing characteristics were assumed. Deposition freezing is calculated using the Meyers et al. (1992) formulation. In this way, the LP parameterization takes into consideration the impact of updraft velocity, w, and aerosol load N_{a} on the number concentration of nucleated ice crystals, $N_{\mathrm{c,nuc}}$. In the cirrus regime, it is capable of calculating $N_{\mathrm{c,nuc}}$ as the result of the competition of both freezing mechanisms. For temperatures above T_{hom}, homogeneous freezing is inactive, and $N_{\mathrm{c,nuc}}$ is given solely by heterogeneous nucleation. However, because the scheme obtains the number of nucleated ice crystals from curve-fitted functions of temperature and vertical velocity, these specific equations may not hold as well when extrapolated beyond the curve-fit data domain, nor be applied to aerosols that does not follow the prescribed freezing properties used on the simulations.

The implementation of LP in McRAS-AC for mixed-phase clouds ($T_{\mathrm{hom}} < T < 273\,\mathrm{K}$) follows closely that of Liu et al. (2007), and was described and tested in a SCM framework (Bhattacharjee et al., 2010). In this regime, $N_{\mathrm{c,nuc}}$ is calculated by adding the contributions from the the numerical correlations described above and the contribution from deposition freezing as given by a modified version of the Meyers et al. (1992) formula,

$$N_{\mathrm{id}}(S_{\mathrm{i}}) = f(z)N_0\exp(a + b(S_{\mathrm{i}} - 1)) \tag{1}$$

where N_{id} is the number concentration of ice crystals due to deposition nucleation in m^{-3}, $N_0 = 10^{-3}\,\mathrm{m}^{-3}$, $a = -0.639$, and $b = 0.1296$, and $f(z)$ is an empirical height correction factor, given by $f(z) = 10^{(z_0-z)/\delta z}$, with $z_0 = 1\,\mathrm{km}$, $\delta z = 6.7\,\mathrm{km}$, and $f(z) \in [0.12, 1.0]$. This decay factor was derived from observations by Minikin et al. (2003) during the INCA (Interhemispheric Differences in Cirrus Properties from Anthropogenic Emissions) campaign, to augment the formula by Meyers et al. (1992) that was derived from ground-level observations.

In the present work we implemented and tested the BN parameterization in McRAS-AC. BN is based on an analytical solution of the governing equations of a cooling air parcel in which deliquesced aerosol and heterogeneous IN are allowed to freeze and grow by water vapor deposition (Barahona and Nenes, 2008, 2009a,b). Accordingly, BN circumvents the need for curve-fitted equations, and holds for a wide range of configurations encountered in the physical system. The availability of IN in the BN parameterization can be described, in principle, with any heterogeneous nucleation parameterizations. Here we use the correlations of Meyers et al. (1992) (MY92), Phillips et al. (2008) (PDA08), and the semi-empirical spectra derived from classical nucleation theory of Barahona and Nenes (2009b), (CNT_BN). MY92 is a widely used, empirical IN spectrum which depends only on S_{i}. PDA08 is also empirical however it separately considers the contribution of organics, dust, and black carbon to the IN population.

CNT_BN is based on an approximation of classical nucleation theory to scale observed IN concentration as a function of supersaturation. For temperatures $T < T_{\mathrm{hom}}$, BN calculates the competing effects of homogeneous nucleation on deliquesced aerosol and the heterogeneous freezing for the availability of water vapor in a forming cirrus cloud. The maximum supersaturation with respect to ice attained in the ascending parcel, $S_{\mathrm{i,max}}$, is calculated by balancing the depletion effect from deposition growth of ice crystals and the availability of water vapor from cooling. In this way, $S_{\mathrm{i,max}}$ is given by the dynamics of cooling and ice nucleation. BN then uses the maximum saturation to calculate $N_{\mathrm{c,nuc}}$.

The application of BN in the mixed-phase cloud regime differs slightly from that of LP. In the absence of any liquid water, the maximum supersaturation in the parcel would be dictated dynamically by expansion cooling and by the IN concentration. However, in McRAS-AC, any initial condensate is considered to be liquid (Rotstayn, 1997) and its then partitioned following Rotstayn et al. (2000). Therefore, in practice, ice nucleation above T_{hom} is assumed to occur in an environment saturated with respect to water. Under this circumstance, $S_{\mathrm{i,max}}$ is fixed by the assumption of water saturation, equal to $S_{\mathrm{i,max}} = e_{\mathrm{sw}}(T)/e_{\mathrm{si}}(T)$, i.e., the ratio of the saturation vapor pressure over water and over ice, and it is therefore independent of the dynamic forcing, w, or aerosol loading. The number concentration of nucleated ice crystals, $N_{\mathrm{c,nuc}}$, is then calculated by direct application of the IN spectra at the given $S_{\mathrm{i,max}}$.

2.2 McRAS-AC cold and mixed-phase cloud microphysics

The cloud microphysics in McRAS-AC include balance equations for the mixing ratios of liquid water, q_{l}, and cloud ice q_{i}. The precipitation microphysics are described by Sud and Lee (2007), which recast Seifert and Beheng (2006) to apply it to the thicker clouds of a coarse resolution GCM. The activation of aerosol to cloud droplets follows the parameterization of Fountoukis and Nenes (2005). Aerosol mass concentrations are taken from the Goddard Chemistry Aerosol Radiation and Transport (GOCART), and log-normal size distribution for each species are prescribed.

The partitioning of cloud condensate between ice and liquid in mixed-phase clouds is prognostic, and takes into account the Bergeron-Findeisen (BF) process, by which cloud droplets evaporate and the resulting water vapor deposits, to ice crystals. The process is represented following Rotstayn et al. (2000), which explicitly accounts for the dependence of the ice deposition rate on crystal number concentration, N_c.

Ice crystal number concentration N_c is determined in McRAS-AC by the processes of ice nucleation, contact freezing, and by melting of cloud ice. The ice nucleation term is calculated with the LP and the BN parameterizations as explained in Sect. 2.1. Contact freezing of supercooled cloud droplets through Brownian coagulation with insoluble IN (mineral dust) is included as given by Young (1974).

Aerosol input for ice nucleation is also based on GOCART aerosol climatology. A single mode log-normal size distribution was assumed for black carbon, with geometrical mean diameter, $d_g = 0.04\,\mu\text{m}$, and a geometric standard deviation $\sigma_g = 2.3$ (Jensen and Toon, 1994). Similarly, sulfate aerosol size distribution is assumed log-normal with $d_g = 0.14\,\mu\text{m}$ and $\sigma_g = 1.5$ (Pueschel et al., 1992). The density of black carbon was assumed equal to $1\,\text{g}\,\text{cm}^{-3}$ while for sulfates, we assumed the density of sulfuric acid ($1.84\,\text{g}\,\text{cm}^{-3}$). A probability distribution function of cloud scale vertical velocity, w, was used to represent the local variations of velocity at scales relevant for nucleation. The distribution was assumed to be a normal distribution with a fixed standard deviation of $0.25\,\text{m}\,\text{s}^{-1}$, consistent with observations in the INCA campaign (Kärcher and Ström, 2003).

2.3 Forcing data

The SCM configuration consists of an isolated column of a global circulation model, and is therefore, a 1-dimensional time-dependent atmospheric model. The lateral forcing fields to the 72 pressure levels in the atmospheric columns of GEOS-5 are prescribed from assimilated 4-D observational data. For the purpose of this study, we used the forcing from the TWP-ICE intensive observation period (IOP), derived by the

Atmospheric Radiation Measurement (ARM) program. It includes data from 17 January to 12 February 2006. This data set has been previously utilized in forcing SCM simulations with the intent of testing ice microphysics for GCMs (Wang et al., 2009a), as well as for comparing simulations produced with bulk microphysical schemes of varying complexity in a cloud resolving model with observational data (Wang et al., 2009b; Lee and Donner, 2011). The TWP-ICE data is ideally suited for testing the representation of cold and mixed-phase clouds in models and is an often used test case that allows comparison with other existing studies (e.g., Varble et al., 2011; Fridlind et al., 2012). It includes periods dominated by deep convective clouds and by persisting layers of cirrus clouds.

3 Simulated clouds fields

Table 1 summarizes the simulations considered in this study. The objective of the simulation experiments is to evaluate the sensitivity of the cloud fields to the treatment of ice nucleation. A "control" simulation was performed with the LP ice nucleation parameterization as described above, which has been used in the McRAS-AC framework before (Bhattacharjee et al., 2010). Other simulation experiments were carried out with the BN parameterization, utilizing three different IN spectra. Two additional simulations were considered, in which the contribution to N_c from contact freezing was neglected (LP-NoFrzc and BN-PDA08-NoFrzc). All the simulations share the same lateral forcing fields, surface fluxes, and aerosol input, and they only differ on the treatment of ice formation.

The time-height distributions of the total cloud fraction, CF, exhibits the basic features observed during the TWP-ICE campaign (Fig. 1). In the first period of the intensive observation period (IOP), prior to 25 January 2006, the region was influenced by an active monsoon period characterized by considerable convective activity. From 26 January to 2 February, the monsoon was suppressed, and little convective activity was observed, but high clouds persisted through the period. In the final part of the IOP

(3–13 February) the region was increasingly impacted by continental storms, reflected in a renewed increase in the convective activity.

The simulated cloud fields show some differences in the CF, particularly the simulation with the BN-PDA08, which shows higher frequency of high CF cells. Common to all the simulations with the BN scheme is an increase in the CF for the mixed-phase regime as compared with the LP-CTRL simulation, particularly in the convectively active periods, as shown for two of the simulations in Fig. 3. The resulting simulated q_i fields are shown in Fig. 2. Ice mixing ratios generally reach a maxima in the layer extending from the 0 °C to the −38 °C levels. The overall ice mixing ratios encountered in the LP-CTRL simulation are generally higher than for the BN cases, the difference being more pronounced for the mixed-phase regime.

The temperature dependence of $N_\mathrm{c,nuc}$ and the total ice crystal concentration N_c was calculated from the model output for each one of the simulations as a function of temperature (Fig. 4). The impact of the nucleation scheme in the partitioning of condensate was investigated through the ice fraction, f_c, defined as

$$f_\mathrm{c} = \frac{q_\mathrm{i}}{q_\mathrm{i} + q_\mathrm{l}}. \qquad (2)$$

Figure 5 shows the temperature dependence of the condensate partitioning, for the BN-PDA08, LP-CTRL, BN-PDA08-NoFrzc, and LP-NoFrzc. Attention was given to variables affecting the radiative properties of the ice clouds. The size of ice particles would be among the most directly affected variables with changes in crystal concentrations. The behavior of effective radius for ice particles as a function of temperature is shown in Fig. 6 for two of the simulations. Figure 7 shows a time series of IWP from different simulation experiments, together with IWP derived from satellite retrievals using the Visible Infrared Shortwave-Infrared Split-Window Techinique (VISST), described in Fridlind et al. (2012).

4 Discussion of the results

Since the lateral forcing and surface fluxes were prescribed identically in all simulation experiments, any differences in the cloud fields can be attributed to the interaction of the ice nucleation scheme with the BF process and the cloud microphysical response that follows. Some such differences are encountered between the fields produced with LP and BN parameterization, respectively. $N_{\mathrm{c,nuc}}$ calculated with BN is systematically lower for the mixed-phase cloud regime irrespective of the heterogeneous nucleation scheme used, however, the difference is greater between LP-CTRL and BN-PDA08, for which the maximum difference in the predicted $N_{\mathrm{c,nuc}}$ can be considerable (Fig. 4). The low concentration of IN predicted by the PDA08 spectrum, typically two orders of magnitude lower than produced by the other spectra, explains part of this difference. However, the systematic discrepancy between LP and BN in the mixed-phase regime is likely due to the different implementation of the two nucleation schemes. As described in Sect. 2.1, the LP scheme adds the contributions from immersion freezing (given by the numerical correlations of Liu and Penner, 2005, and from deposition, as given by Eq. 1). In the BN schemes the availability of IN in the mixed-phase regime is dictated by the IN spectrum alone, which consider deposition and condensation freezing.

The large differences in predicted $N_{\mathrm{c,nuc}}$ are also noticeable in the resulting N_{c} fields, but the magnitude of the difference is significantly lower. In the range of temperatures where contact freezing is active ($270.15\,\mathrm{K} > T > 235\,\mathrm{K}$) this mechanism was found to contribute, on average, between $10^{-4}\,\mathrm{cm}^{-3}$ and $10^{-3}\,\mathrm{cm}^{-3}$ to the ice crystal concentration, thereby effectively providing a lower bound for N_{c} (Fig. 4). This contribution is significant only for IN spectrum predicting very low $N_{\mathrm{c,nuc}}$ (such as PDA08), or for the temperatures above $T \sim 260\,\mathrm{K}$, in which the other IN spectrum (MY92 and BN-CNT) predicts very small $N_{\mathrm{c,nuc}}$.

It is expected that the differences in N_{c} would significantly impact other cloud microphysical variables, particularly through the modification of the rate of the BF process. Lower ice crystal concentrations should result in lower rates of conversion of liquid water to ice because the surface area for vapor–ice mass transfer is low (Rotstayn et al., 2000). Such behavior, in which low aerosol concentrations are associated with low f_c, has been observed in satellite retrievals (Choi et al., 2010). However, the ice fraction exhibits little to no change across simulations even for the cases where N_c differ by a factor of 100 (Fig. 5a, b). This diminished sensitivity of f_c to ice crystal concentration seems to be caused by the action of the contact freezing mechanism. To verify this, two simulations in which this mechanism was neglected were performed LP-NoFrzc and BN-PDA08-NoFrzc, (Fig. 5c, d). LP-NoFrzc shows that the transition from pure liquid to pure ice cloud occurs over a larger temperature interval as compared to simulations in which contact freezing is allowed to occur. However, because LP predicts relatively large crystal concentrations in the entire range of supercooling temperatures, the BF process is always fast, resulting in a rather similar dependence of f_c on temperature. This is not the case for the simulations with BN-PDA08, in which the low N_c severely limits the rate of conversion of liquid water to ice by water vapor deposition, which is evidenced when contact freezing is turned off (Fig. 5d). The narrow temperature range associated with the transition from $f_c = 0$ at 273 K to $f_c = 1$ at 260 K when contact freezing was included, is consistent with other studies with the same partitioning scheme, as well as with available cloud observations of f_c (Rotstayn et al., 2000; Liu et al., 2007). The transition to a fully glaciated state which sometimes produces excessive ice cloud at low temperatures could arise from the assumption that the BF mechanism dominates this regime (Korolev, 2007).

The cloud amount in the mixed-phase regime was affected by the crystal ice nucleation parameterization used in the simulations. As shown in Fig. 3, there is an increase in the frequency of occurrence of cloudy cells with $CF > 0.5$ when the BN-PDA08 parameterization is used instead of LP. This is true for the three IN spectra utilized in this study, with CF being 49 % larger for BN-PDA08, and ∼ 25 % for MY92 and BN-CNT, as compared to simulations with LP.

In the cirrus cloud regime, the difference in $N_{c,nuc}$ between LP and BN is less pronounced than in the mixed-phase regime. For this temperature range, crystal concentrations calculated with LP and BN are within one order of magnitude irrespective of the IN spectrum used, which is consistent with the variability reported in previous studies (Barahona et al., 2010). $N_{\mathrm{c,nuc}}$ for LP-CTRL and BN-PDA08 are in close agreement, specially for temperatures above 200 K, however, the predicted mechanism of freezing is different for both parameterizations. Due to the very low IN number predicted with PDA08, the contribution of heterogeneous freezing to $N_{\mathrm{c,nuc}}$ in BN-PDA08 is negligible, and the process is dominated by homogeneous freezing. The opposite behavior is observed when the LP parameterization is used, in which homogeneous freezing only contributes significantly to the $N_{\mathrm{c,nuc}}$ at extremely low temperatures. When BN-CNT or MY92 are used instead, the lower $N_{\mathrm{c,nuc}}$ is the result of the depletion of water vapor from the more numerous IN, and homogeneous freezing is triggered only at temperatures between 200 K and 220 K (Fig. 4).

Finally, even though the impact of N_{c} on the simulated condensate partitioning is small, the different ice crystal concentration predicted with the parameterizations considered in this study considerably impact the cloud radiative properties. For instance, Figs. 2 and 3 shows the ice mixing ratio for different simulation scenarios. The differences observed translate also into ice water path differences, as well as of the hydrometeor sizes. Figure 6 shows the temperature dependence of the median values of the calculated ice effective radius for BN-PDA08 and LP-CTRL. The inset shows a histogram of the frequency distribution of the effective radius for BN-PDA08 and LP only for the rage of mixed-phase temperatures. Due to the much lower N_{c} predicted by PDA08, the effective radius is shifted from a median of 45 µm for BN-PDA08, to a smaller size with a median of 32 µm in the LP-CTRL simulation.

The changes induced in the cloud microphysics by the different IN spectra consequently modify the overall column integrated properties of the cloud fields. Figure 7 illustrate the tendencies in the simulated IWP for the different parameterizations. It is clear that IWP for LP-CTRL is higher than for any simulation with BN, with differences being larger in the periods of convective activity. In fact, the average IWP in the active monsoon period for the LP simulation was found to be 0.30 kg m^{-2}, while it was of 0.22 kg m^{-2} for BN-PDA08, and 0.28 kg m^{-2} for BN-CNT and BN-MY92. In the suppressed period, IWP averaged ~ 0.04 kg m^{-2} in all the simulation experiments. This simulation results compare qualitatively well to the available data of IWP as retrieved from VISST. However, the lower bound in the VISST observations tends to be much lower than simulated IWP, while the peaks during the convective events often exhibit higher values than simulated fields. Ice water path from VISST during the active monsoon period averages 0.25 kg m^{-2} and 0.04 kg m^{-2} for the suppressed period.

5 Summary and conclusions

The ice nucleation parameterization of Barahona and Nenes (2009b) was implemented in the GEOS-5 McRAS-AC cloud scheme and tested in single column mode forced with TWP-ICE campaign data. Three different heterogeneous ice nucleation spectra (PDA08, BN-CNT, and MY92) were used in simulations experiments with the BN parameterization framework. The IN concentration predicted by the spectra used in this study varied greatly, with PDA08 predicting very low IN concentrations of around $\sim 10^{-4}$ cm^{-3}, while MY92 and BN-CNT predicted IN concentrations similar to each other, but generally ~ 100 times larger than PDA08 at any given temperature. These simulation experiments were compared to a control simulation using the LP parameterization, which was found to predict the highest ice crystal concentrations across the simulations.

It was shown that the different schemes used in this study often predicted IN concentrations differing by up to three orders of magnitude. Despite these important differences in IN availability, ice crystal number concentration for cirrus cloud temperatures predicted in all the simulations were found to agree within a factor of 10. However, the mechanism by which these ice crystal are produced is considerably different; N_c computed with LP was dominated by heterogeneous freezing, while simulations with BN transitioned from heterogeneous to homogeneous dominated freezing at higher temperatures.

In the regime of mixed-phase clouds, the variations in N_c among simulations with the different nucleation schemes was considerably larger than for the ice-only clouds, with the largest variations being within a factor of ~ 100 in some cases. This larger variability is not surprising, since in the absence of homogeneous freezing, the nucleation schemes strongly depend on the IN nucleation spectra. However, the contribution to N_c from contact freezing of cloud droplets with dust particles of $\sim 10^{-3}\,\mathrm{cm}^{-3}$ provided a lower bound on N_c, and was effectively the largest contributor to crystal concentration when the PDA08 scheme was used. This contribution to N_c also acted to counteract the very large variations in predicted IN concentrations.

Similarly, it was also found that the action of contact freezing efficiently transforming cloud water into cloud ice buffered the impact of the large variations of N_c seen across the different simulation experiments on the partitioning of cloud condensate. Ice mixing ratios, however, where strongly affected by the ice nucleation scheme. Accordingly, cloud microphysical variables relevant to radiative properties, such as the effective radius of ice crystals and the ice water path, were impacted by the wide range of N_c predicted. It was observed that nucleation schemes that predict lower N_c lead to lower in-cloud ice mixing ratios and ice water path, and considerably larger crystal sizes.

This study highlights the need for detailed cloud microphysical observations to constrain the large uncertainties associated with the ice nucleation process which limit the ability of GCM models to make accurate estimates of the contribution of cold clouds to the overall aerosol indirect effects. Continued development and refinement of ice nucleation schemes capable of accounting correctly for different freezing mechanisms is needed; using the approaches used here will help accomplish this.

Acknowledgements. R. Morales-Betancourt acknowledges the JCET/NASA Graduate Summer Research Program in Earth Sciences. A. Nenes acknowledges support from DOE contract DE-SC0007145 and NASA ACMAP contract NNX08AK50G. D. Barahona was supported by the NASA Modeling, Analysis, and Prediction program under WBS 802678.02.17.01.07.

References

Barahona, D.: On the ice nucleation spectrum, Atmos. Chem. Phys., 12, 3733–3752, doi:10.5194/acp-12-3733-2012, 2012. 14931

Barahona, D. and Nenes, A.: Parameterization of cirrus cloud formation in large-scale models: homogeneous nucleation, J. Geophys. Res., 113, D11211, doi:10.1029/2007JD009355, 2008. 14934, 14935

Barahona, D. and Nenes, A.: Parameterizing the competition between homogeneous and heterogeneous freezing in cirrus cloud formation – monodisperse ice nuclei, Atmos. Chem. Phys., 9, 369–381, doi:10.5194/acp-9-369-2009, 2009a. 14934, 14935, 14950

Barahona, D. and Nenes, A.: Parameterizing the competition between homogeneous and heterogeneous freezing in ice cloud formation – polydisperse ice nuclei, Atmos. Chem. Phys., 9, 5933–5948, doi:10.5194/acp-9-5933-2009, 2009b. 14931, 14932, 14933, 14934, 14935, 14943

Barahona, D., Rodriguez, J., and Nenes, A.: Sensitivity of the global distribution of cirrus ice crystal concentration to heterogeneous freezing, J. Geophys. Res., 115, D23213, doi:10.1029/2010JD014273, 2010. 14933, 14942

Bhattacharjee, P. S., Sud, Y. C., Liu, X., Walker, G. K., Yang, R., and Wang, J.: Importance of including ammonium sulfate ($(NH_4)_2SO_4$) aerosols for ice cloud parameterization in GCMs, Ann. Geophys., 28, 621–631, doi:10.5194/angeo-28-621-2010, 2010. 14934, 14935, 14938

Choi, Y.-S., Lindzen, R. S., Ho, C.-H., and Kim, J.: Space observations of cold-cloud phase change, P. Natl. Acad. Sci. USA, 107, 11211–11216, doi:10.1073/pnas.1006241107, 2010. 14941

Curry, J. A. and Khvorostyanov, V. I.: Assessment of some parameterizations of heterogeneous ice nucleation in cloud and climate models, Atmos. Chem. Phys., 12, 1151–1172, doi:10.5194/acp-12-1151-2012, 2012. 14932

DelGenio, A., Yao, M. W. K., and Lo, K.: A prognostic cloud water parameterization for global climate models, J. Climate, 9, 270–304, 1996. 14930

Fountoukis, C. and Nenes, A.: Continued development of a cloud droplet formation parameterization for global climate models, J. Geophys. Res., 110, D11212, doi:10.1029/2004JD005591, 2005. 14936

Fridlind, A. M., Ackerman, A. S., Chaboureau, J.-P., Fan, J., Grabowski, W. W., Hill, A. A., Jones, T. R., Khaiyer, M. M., Liu, G., Minnis, P., Morrison, H., Nguyen, L., Park, S., Petch, J. C., Pinty, J.-P., Schumacher, C., Shipway, B. J., Varble, A. C., Wu, X., Xie, S., and Zhang, M.: A comparison of TWP-ICE observational data with cloud-resolving model results, J. Geophys. Res., 117, D05204, doi:10.1029/2011JD016595, 2012. 14938, 14939

Hoose, C., Kristjánsson, J. E., Chen, J.-P., and Hazra, A.: A classical-theory-based parameterization of heterogeneous ice nucleation by mineral dust, soot, and biological particles in a global climate model, J. Atmos. Sci., 67, 2483–2503, doi:10.1175/2010JAS3425.1, 2010. 14932

Intergovernmental Panel on Climate Change: Fourth Assessment Report: Climate Change 2007: Working Group I Report: The Physical Science Basis, Geneva, IPCC, 2007. 14930

Jensen, E. J. and Toon, O. B.: Ice nucleation in the upper troposphere: sensitivity to aerosol number density, temperature, and cooling rate, Geophys. Res. Lett., 21, 2019–2022, 1994. 14937

Kärcher, B. and Lohmann, U.: A parameterization of cirrus cloud formation: homogeneous freezing of supercooled aerosols, J. Geophys. Res., 107, 4010, doi:10.1029/2001JD000470, 2002. 14932

Kärcher, B. and Lohmann, U.: A parameterization of cirrus cloud formation: heterogeneous freezing, J. Geophys. Res., 108, 4402, doi:10.1029/2002JD003220, 2003. 14932

Kärcher, B. and Ström, J.: The roles of dynamical variability and aerosols in cirrus cloud formation, Atmos. Chem. Phys., 3, 823–838, doi:10.5194/acp-3-823-2003, 2003. 14937

Khvorostyanov, V. I. and Curry, J. A.: Critical humidities of homogeneous and heterogeneous ice nucleation: inferences from extended classical nucleation theory, J. Geophys. Res., 114, D04207, doi:10.1029/2008JD011197, 2009. 14931

Korolev, A.: Limitations of the Wegener-Bergeron-Findeisen mechanism in the evolution of mixed-phase clouds, J. Atmos. Sci., 64, 3372–3375, doi:10.1175/JAS4035.1, 2007. 14932, 14941

Lee, S. S. and Donner, L. J.: Effects of cloud parameterization on radiation and precipitation: a comparison between single-moment microphysics and double-moment microphysics, Terr. Atmos. Ocean. Sci., 22, 403–420, doi:10.3319/TAO.2011.03.03.01(A), 2011. 14938

Lin, R.-F., Starr, D. O., DeMott, P. J., Cotton, R., Sassen, K., Jensen, E., Kärcher, B., and Liu, X.: Cirrus Parcel Model Comparison Project. Phase 1: The critical components to simulate cirrus initiation explicitly, J. Atmos. Sci., 59, 3641–3659, 2002. 14932

Liu, X. and Penner, J. E.: Ice nucleation parameterization for global models, Meteorol. Z., 14, 499–514, 2005. 14932, 14934, 14940, 14950

Liu, X., Penner, J. E., Ghan, S. J., and Wang, M.: Inclusion of ice microphysics in the NCAR Community Atmospheric Model Version 3 (CAM3), J. Climate, 20, 4526–4547, doi:10.1175/JCLI4264.1, 2007. 14931, 14932, 14935, 14941

Lohmann, U.: Possible aerosol effects on ice clouds via contact nucleation, J. Atmos. Sci., 59, 647–656, 2002. 14930

Lohmann, U. and Diehl, K.: Sensitivity studies of the importance of dust ice nuclei for the indirect aerosol effect on stratiform mixed-phase clouds, J. Atmos. Sci., 63, 968–982, 2005. 14930

Lohmann, U. and Feichter, J.: Global indirect aerosol effects: a review, Atmos. Chem. Phys., 5, 715–737, doi:10.5194/acp-5-715-2005, 2005. 14930

May, P. T., Mather, J. H., Vaughan, G., and Jakob, C.: Field research: characterizing oceanic convective cloud systems, B. Am. Meteorol. Soc., 89, 153–155, doi:10.1175/BAMS-89-2-153, 2008. 14933

Meyers, M., DeMott, P. J., and Cotton, W. R.: New primary ice-nucleation parameterizations in an explicit cloud model, J. Appl. Meteorol., 31, 708–721, 1992. 14931, 14934, 14935, 14950

Minikin, A., Petzold, A., Ström, J., Krejci, R., Seifert, M., Veltoven, P., Schlager, H., and Schumann, U.: Aircraft observations of the upper tropospheric fine particle aerosol in the Northern and Southern Hemispheres at midlatitudes, Geophys. Res. Lett., 30, 1503–1506, doi:10.1029/2002GL016458, 2003. 14935

Morrison, H. and Gettelman, A.: A new two-moment bulk stratiform cloud microphysics scheme in the Community Atmosphere Model, Version 3 (CAM3). Part I: Description and numerical tests, J. Climate, 21, 3642–3659, doi:10.1175/2008JCLI2105.1, 2008. 14931

Muhlbauer, A. and Lohmann, U.: Sensitivity studies of aerosol–cloud interactions in mixed-phase orographic precipitation, J. Atmos. Sci., 66, 2517–2538, doi:10.1175/2009JAS3001.1, 2009. 14931

Penner, J. E., Quaas, J., Storelvmo, T., Takemura, T., Boucher, O., Guo, H., Kirkevåg, A., Kristjánsson, J. E., and Seland, Ø.: Model intercomparison of indirect aerosol effects, Atmos. Chem. Phys., 6, 3391–3405, doi:10.5194/acp-6-3391-2006, 2006. 14930

Phillips, V. T. J., Donner, L. J., and Garner, S. T.: Nucleation processes in deep convection simulated by a cloud-system-resolving model with double-moment bulk microphysics, J. Atmos. Sci., 64, 738–761, doi:10.1175/JAS3869.1, 2007. 14931

Phillips, V. T. J., DeMott, P. J., and Andronache, C.: An empirical parameterization of heterogeneous ice nucleation for multiple chemical species of aerosol, J. Atmos. Sci., 65, 2757–2783, doi:10.1175/2007JAS2546.1, 2008. 14931, 14935, 14950

Pruppacher, H. and Klett, J.: Microphysics of Clouds and Precipitation, Atmospheric and Oceanographic Sciences Library, Kluwer Academic Publishers, Dordrecht, 1997. 14930, 14932

Pueschel, R. F., Ferry, G. V., Snetsinger, K. G., Goodman, J., Dye, J. E., Baumgardner, D., and Gandrud, B. W.: A case of type I polar stratospheric cloud formation by heterogeneous nucleation, J. Geophys. Res., 9, 8105–8114, doi:10.1029/91JD02352, 1992. 14937

Rasch, P. J. and Kristjánsson, J. E.: A comparison of the CCM3 model climate using diagnosed and predicted condensate parameterizations, J. Climate, 11, 1587–1614, 1998. 14930

Rotstayn, L. D.: A physically based scheme for the treatment of stratiform precipitation in large-scale models. I: Description and evaluation of the microphysical processes, Q. J. Roy. Meteor. Soc., 123, 1227–1282, 1997. 14936

Rotstayn, L. D., Ryan, B., and Katzfey, J.: A scheme for calculation of the liquid fraction in mixed-phase stratiform clouds in large-scale models, Mon. Weather Rev., 128, 1070–1088, 2000. 14930, 14936, 14937, 14941

Salzmann, M., Ming, Y., Golaz, J.-C., Ginoux, P. A., Morrison, H., Gettelman, A., Krämer, M., and Donner, L. J.: Two-moment bulk stratiform cloud microphysics in the GFDL AM3 GCM: description, evaluation, and sensitivity tests, Atmos. Chem. Phys., 10, 8037–8064, doi:10.5194/acp-10-8037-2010, 2010. 14931, 14932

Seifert, A. and Beheng, K. D.: A double-moment parameterization for simulating autoconversion, accretion and selfcollection, Meteorol. Atmos. Phys., 59, 265–281, 2001. 14931

Seifert, A. and Beheng, K. D.: A two-moment cloud microphysics parameterization for mixed-phase clouds. Part 1: Model description, Meteorol. Atmos. Phys., 92, 45–66, doi:10.1007/s00703-005-0112-4, 2006. 14931, 14936

Storelvmo, T., Kristjánsson, J. E., and Lohmann, U.: Aerosol influence on mixed-phase clouds in CAM-Oslo, J. Atmos. Sci., 65, 3214–3230, doi:10.1175/2008JAS2430.1, 2008. 14932

Sud, Y. C. and Lee, D.: Parameterization of aerosol indirect effect to complement McRAS cloud scheme and its evaluation with the 3-year ARM-SGP analyzed data for single column models, Atmos. Res., 86, 105–125, 2007. 14931, 14932, 14933, 14934, 14936

Sud, Y. C. and Walker, G. K.: Microphysics of clouds with the relaxed arakawa-schubert scheme (McRAS). Part I: Design and evaluation with GATE Phase III data, J. Atmos. Sci., 56, 3196–3220, doi:10.1029/2008GL036817, 1999. 14934

Varble, A., Fridlind, A. M., Zipser, E. J., Ackerman, A. S., Chaboureau, J.-P., Fan, J., Hill, A., McFarlane, S. A., Pinty, J.-P., and Shipway, B.: Evaluation of cloud-resolving model intercomparison simulations using TWP – ICE observations: precipitation and cloud structure, J. Geophys. Res., 116, D12206, doi:10.1029/2010JD015180, 2011. 14938

Wang, W., Liu, X., Xie, S., Boyle, J., and McFarlane, S. A.: Testing ice microphysics parameterizations in the NCAR Community Atmospheric Model Version 3 using Tropical Warm Pool International Cloud Experiment data, J. Geophys. Res., 114, D14107, doi:10.1029/2008JD011220, 2009a. 14938

Wang, Y., Long, C., Leung, L., Dudhia, J., McFarlane, S., Mather, J., Ghan, S. J., and Liu, X.: Evaluating regional cloud-permitting simulations of the WRF model for the Tropical Warm Pool International Cloud Experiment (TWP-ICE), Darwin, 2006, J. Geophys. Res., 114, D21203, doi:10.1029/2009JD012729, 2009b. 14938

Young, K. C.: The role of contact nucleation in ice phase initiation in clouds, J. Atmos. Sci., 31, 768–776, 1974. 14937

Table 1. Simulations reported in this study. The simulation set-up for all the simulations is identical, and they only differ on the ice nucleation scheme.

Simulation ID	Contact Freezing	Ice-only Clouds (cirrus)	Mixed-Phase Clouds
LP-CTRL	Yes	Liu and Penner (2005)	Meyers et al. (1992)
LP-NoFrzc	No	Liu and Penner (2005)	Meyers et al. (1992)
BN-PDA08	Yes	Barahona and Nenes (2009a)	Phillips et al. (2008)
BN-PDA08-NoFrzc	No	Barahona and Nenes (2009a)	Phillips et al. (2008)
BN-CNT	Yes	Barahona and Nenes (2009a)	Barahona and Nenes (2009a)
BN-MY92	Yes	Barahona and Nenes (2009a)	Meyers et al. (1992)

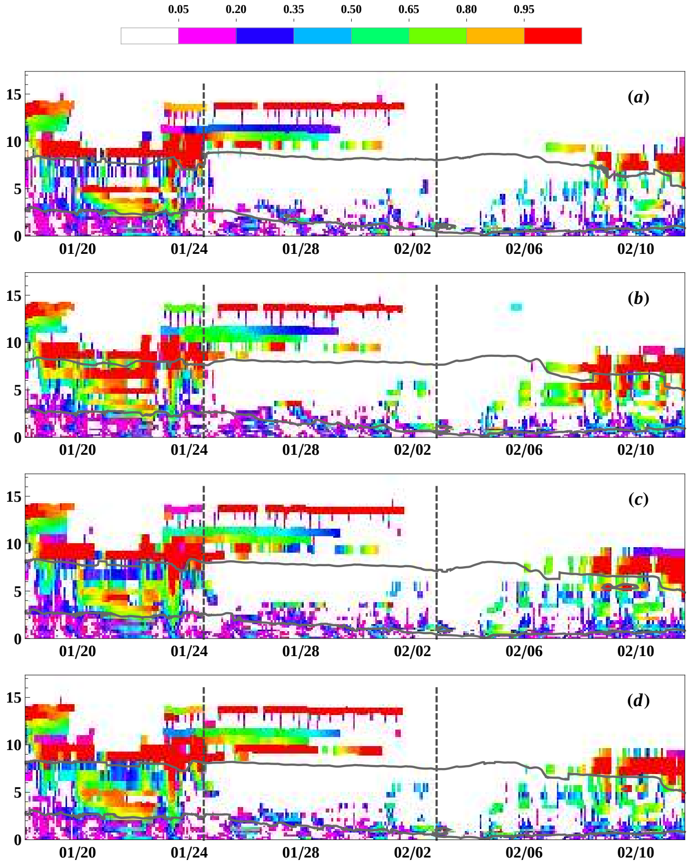

Fig. 1. Time-Height distribution of the simulated cloud fraction for **(a)** control simulation with the LP ice nucleation parameterization. **(b)** Simulation with BN and the PDA08 ice nucleation spectra. **(c)** Simulation BN and the CNT ice nucleation spectra. **(d)** Simulation BN09 with the MY92 ice nucleation spectra. The gray contours correspond to the 0 °C and −38 °C isolines, indicating the region where mixed-phase clouds may occur.

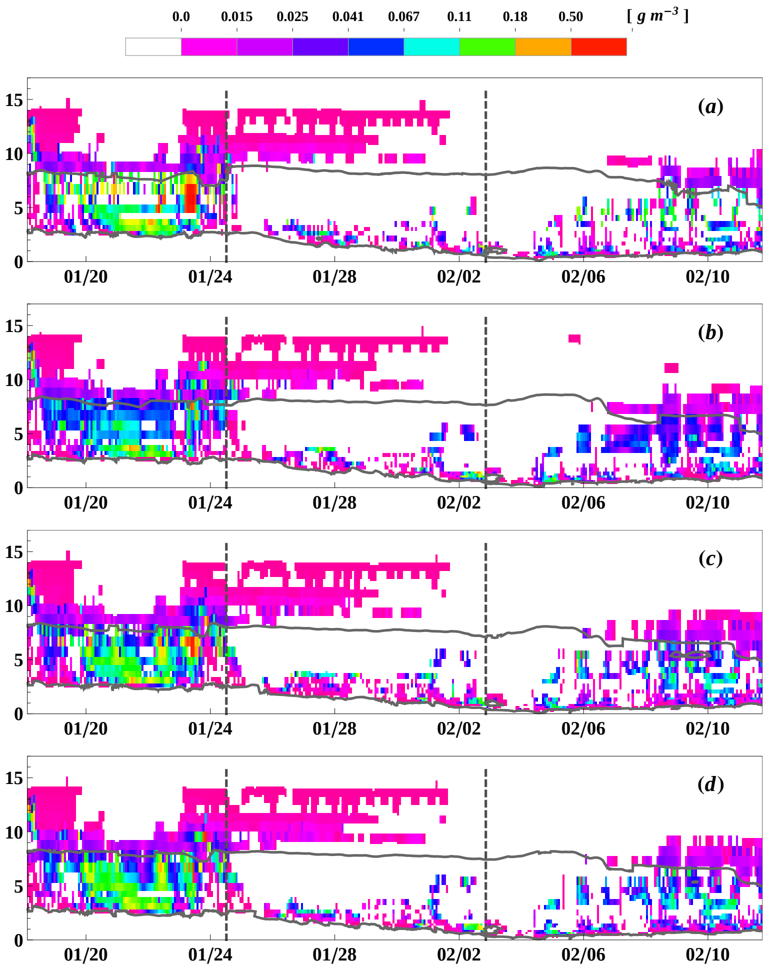

Fig. 2. As in Fig. 1 but for ice mixing ratio in ($\mathrm{g\,m^{-3}}$).

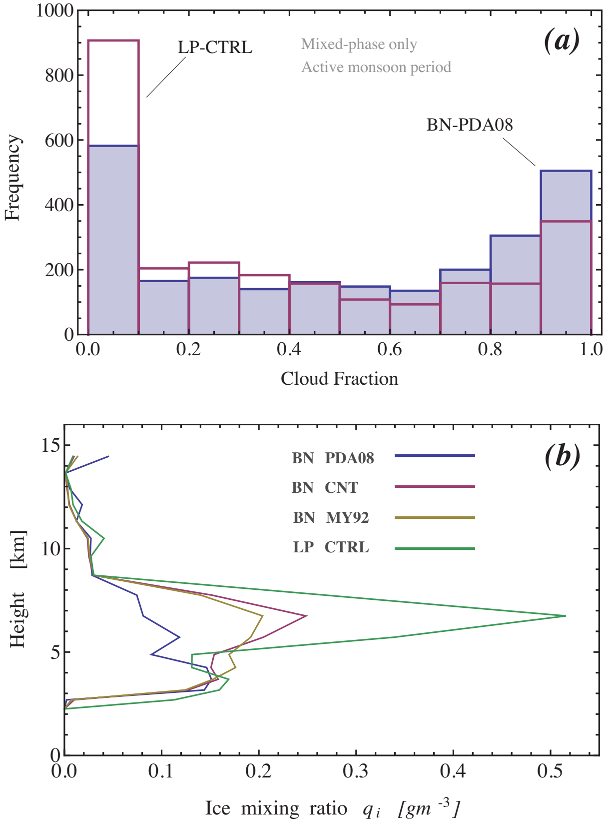

Fig. 3. (a) Histogram of cloud fraction for the LP-CTRL and BN-PDA08 simulations. The frequencies are calculated for the active monsoon period and for cells with temperatures in the range $235\,\mathrm{K} > T > 273\,\mathrm{K}$. **(b)** Vertical profile of in-cloud ice mixing ratios averaged over the monsoon active period.

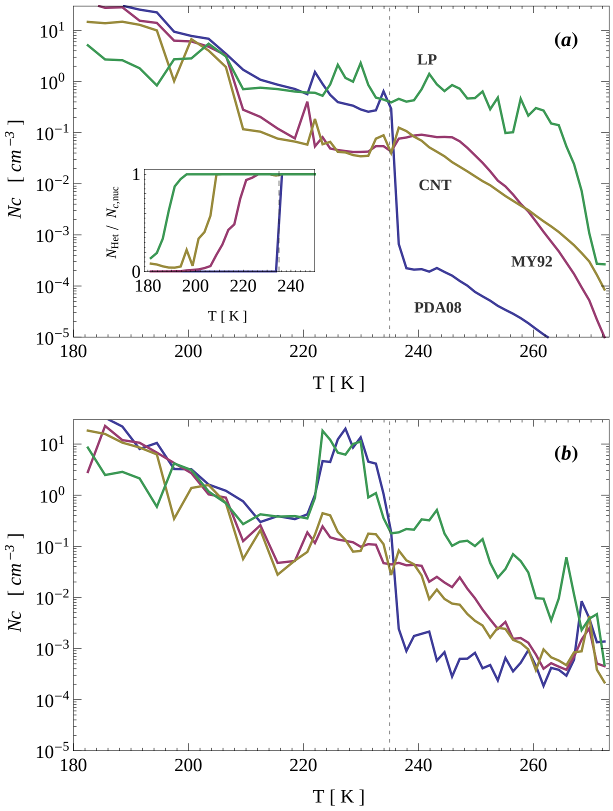

Fig. 4. (a) Average number of nucleated ice crystals, $N_{\mathrm{c,nuc}}$ as a function of temperature for the simulations considered in this study. The inset is the fraction of crystals nucleated heterogeneously, $N_{\mathrm{het}}/N_{\mathrm{c,nuc}}$. **(b)** Average number concentration of ice crystals N_{c} as a function of temperature. The vertical dashed line marks the homogeneous freezing temperature threshold.

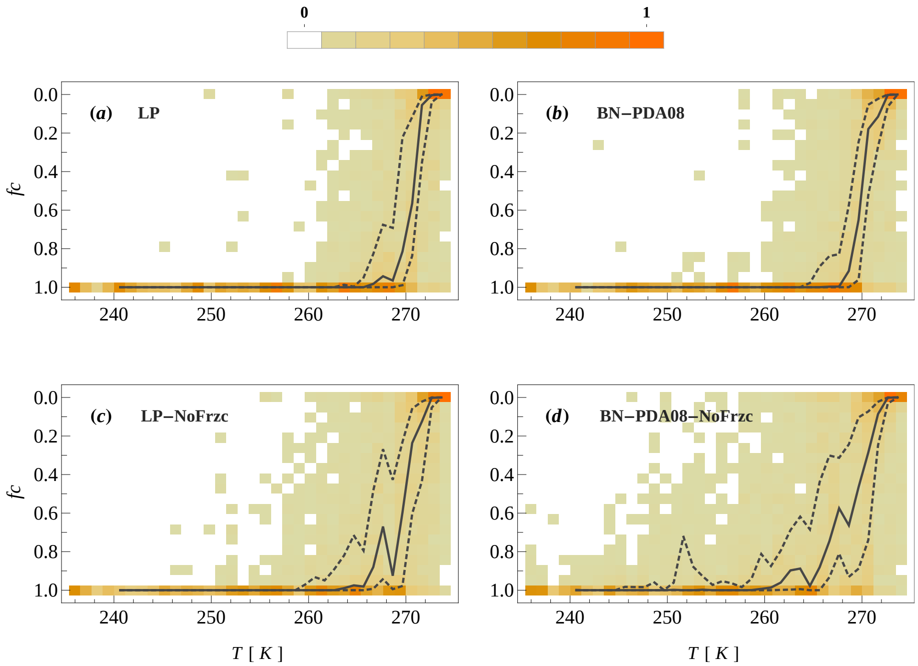

Fig. 5. Frequency distribution of the ice fraction f_c as a function of temperature. The dark gray lines represent the quartiles of the distribution of f_c corresponding to a temperature interval of 1 K. **(a)** LP-CTRL simulation, **(b)** LP-NoFrzc simulation, **(c)** BN-PDA08 simulation, and **(d)** the BN-PDA08-NoFrzc.

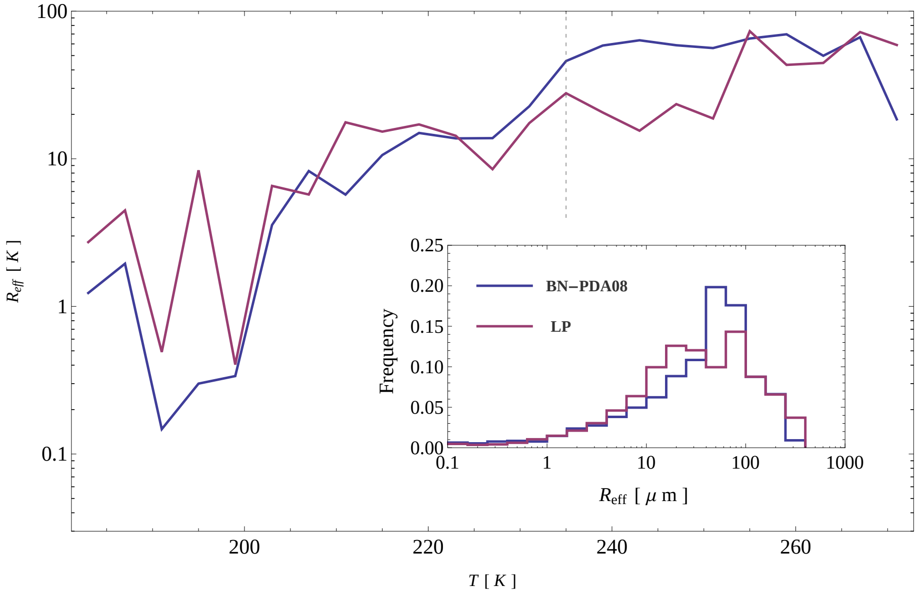

Fig. 6. Median values for the ice crystals effective radius for BN-PDA08 and LP-CTRL. The inset is a histogram of the frequency distribution of the effective radius of ice crystals for the simulated clouds in the mixed-phase temperature regime (235 K < T < 273 K). The bins are uniformly separated in logarithmic scale.

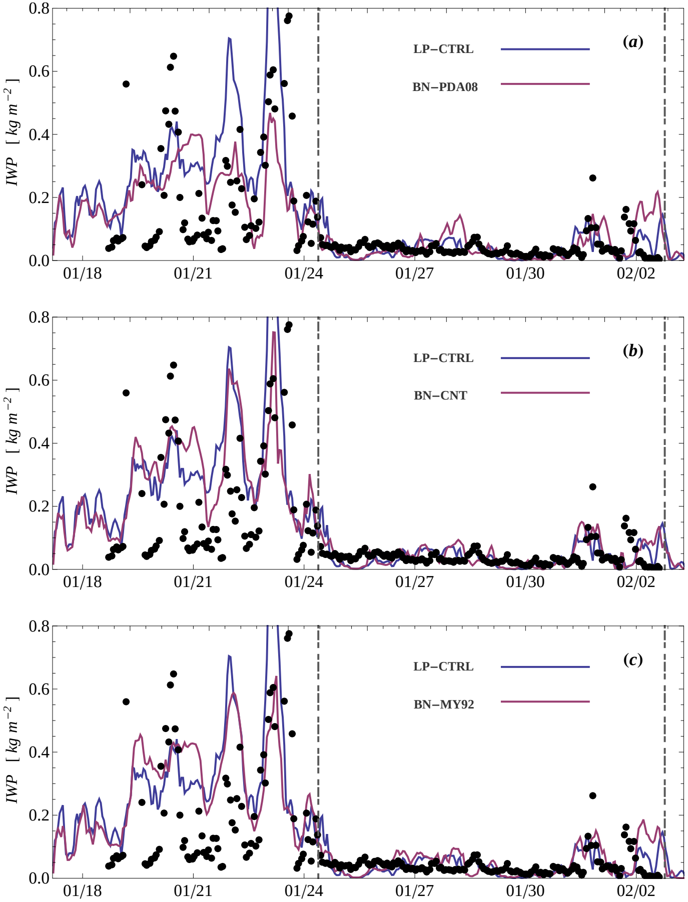

Fig. 7. Ice Water Path (IWP) in kg m^{-2} from VISST data, and simulated IWP for different IN spectra **(a)** LP-CTRL and BN-PDA08, **(b)** LP-CTRL and BN-CNT, **(c)** LP-CTRL and BN-MY92. The dashed vertical lines denote the initiation and end of the suppressed monsoon period.